Contrib Mineral Petrol (1987) 96:391–405

Contributions to Mineralogy and Petrology

Hydrothermal alteration of granite by meteoric fluid: an example from the Carnmenellis Granite, United Kingdom

David Savage, Mark R. Cave, Antoni E. Milodowski, and Ian George
Fluid Processes Research Group, British Geological Survey, Keyworth, Notts NG12 5GG, UK

Abstract. The interaction of granitic rock with meteoric fluid is instrumental in determining the chemistry of pore fluids and alteration mineralogy in downflow portions of convective groundwater circulation cells associated with many hydrothermal systems in the continental crust. Hydrothermal experiments and a detailed mineralogical study have been carried out to investigate the hydrothermal alteration of the Carnmenellis Granite, Cornwall, UK. Samples of drill chippings from a borehole 2 km deep in the Carnmenellis Granite have been reacted with a dilute $Na-HCO_3-Cl$ fluid in hydrothermal solution equipment at temperatures of 80°, 150° and 250° C and a pressure of 50 MPa, with a water/rock mass ratio of 10, for experiment durations up to 200 days. Fluid samples were analysed for seventeen different chemical components, and solids were examined prior to, and after reaction using SEM, electron microprobe and conventional light optic techniques. Experimental fluids were mildly alkaline (pH 7–8.5) and of low salinity (TDS $< 800\ mgl^{-1}$). Mineral-fluid reaction was dominated by the dissolution of plagioclase and the growth of smectite, calcite (at all temperatures), laumontite (at 150° C), wairakite and anhydrite (at 250° C). Final fluids were saturated with respect to quartz and fluorite. Certain trace elements (Li, B, Sr) were either incorporated into solids precipitated during the experiments or sorbed onto mineral surfaces and cannot be considered as 'conservative' (partitioned into the fluid phase) elements. Concentrations of all analysed chemical components showed net increases during the experiments except for Ca (at 250° C) and Mg (at all temperatures). A comparison of the alteration mineralogy observed in the experiments with that present as natural fracture infills in drillcore from the Carnmenellis Granite reveals that the solid products from the experiments correspond closely to mineral assemblages identified as occurring during the later stages of hydrothermal circulation associated with the emplacement of the granite.

Introduction

The investigation of the interaction of meteoric groundwater with granite is relevant to the understanding of the geochemical evolution of many hydrothermal systems. These interactions are fundamental in governing the pore-fluid chemistry and the mineralogy of alteration products in such systems. Experimental studies of such processes provide a link between fluid-phase chemistry and the mineralogy of alteration products which may be lacking from investigations associated with active geothermal wells or fossil hydrothermal systems. For example, laboratory investigations of hydrothermal basalt-seawater interactions (Bischoff and Dickson 1975; Mottl and Holland 1978; Seyfried and Janecky 1983) have been instrumental in elucidating geochemical processes within submarine hydrothermal systems. However, it is also important to emphasise the often non-equilibrium nature of low temperature (< 300° C) water-rock reactions which inevitably limits the applicability of short-term laboratory experiments to an understanding of geological processes.

This study concerns experimental and mineralogical work designed to detail the interaction of meteoric groundwater with granitic rock under hydrothermal conditions and forms part of a broader geochemical, isotopic and mineralogical investigation of rock-water interaction associated with the Carnmenellis Granite, Cornwall, UK carried out by the British Geological Survey, Camborne School of Mines and the University of Bath. Brief descriptions of particular aspects of this work are published elsewhere (Savage et al. 1985, 1986).

Similar experiments in which granite reacts with dilute fluids include those of: R.W. Charles and co-workers in an investigation of the geochemistry of the Fenton Hill Hot Dry Rock geothermal project (Charles 1978; Charles and Bayhurst 1983); J.D. Byerlee and co-workers who examined permeability changes associated with granite-water reactions (Morrow et al. 1981; Moore et al. 1983); Bourg et al. (1985) and Savage (1986) who have examined granite-water reactions with respect to the disposal of high-level radioactive waste.

The Carnmenellis Granite

The Carnmenellis Granite is one of a number of cupola structures, demonstrably connected at depth to form part of a batholith 200 km long, intruded into Devonian sediments some 290 Ma ago (Fig. 1). The batholith is essentially post-tectonic, although its origin as a S- or I-type granite (Chappell and White 1974) is somewhat equivocal (Watson et al. 1984). The granite is a biotite adamellite which may contain megacrysts (porphyroblasts) of potassium feldspar in its surface outcrops but becomes more equigranular with depth (A. Bromley, personal communication). The granite is rich in boron, lithium, fluorine and chlorine, and hydrothermal veins containing Sn, Cu, Pb and Zn minerals occur locally. Charoy (1986), has recently described the petrogenesis of

Offprint requests to: D. Savage

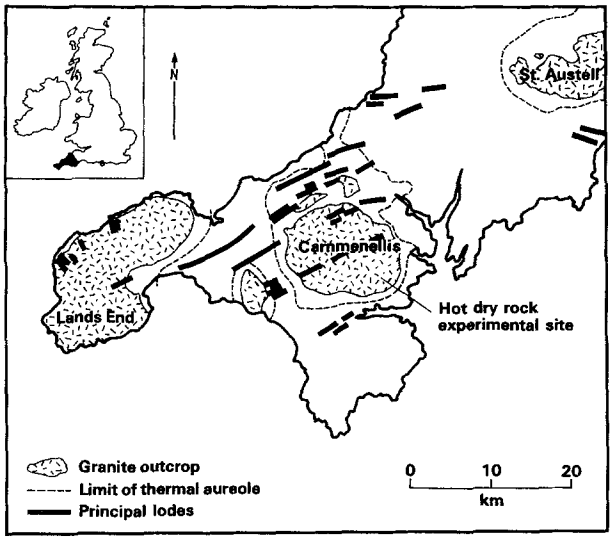

Fig. 1. Location of the Carnmenellis Granite

the Carnmenellis Granite and has suggested an origin by partial melting of pelitic gneisses at 800° C and 5 kb with a water content of approximately 4 wt%. He has ascribed the homogeneity of the pluton to 'hydrothermal reworking' involving re-distribution of Na, K, Fe, Mg, Li, F, B and Rb. The Carnmenellis Granite has an average heat-flow of 120 mW m^{-2} (Tammemagi and Wheildon 1974, 1977), which is considerably greater than the average for the UK. The thermal gradient within the granite is approximately 30° C km^{-1}. As a consequence of the heat flow and the thermal gradient, the granite is the site of a Hot Dry Rock geothermal energy experiment at Rosemanowes Quarry near Camborne (Batchelor 1984) which currently involves injection and production wells at depths of 2–2.5 km, where ambient temperatures are in the range 80°–100° C. A description of the geochemistry of the circulation system is given in McCartney (1984) and Edmunds et al. (1985).

The granite also contains the only thermal groundwaters (up to 52° C) known to occur in granites in the UK. The groundwaters are often saline with total dissolved solids up to 19300 mg l^{-1}, and are unusually enriched in Li which may range up to 125 mg l^{-1} (Edmunds et al. 1984, 1985, in press). Isotopic evidence suggests that the groundwaters are 95% meteoric in origin, which precludes any major contribution from seawater. Edmunds et al. (1984, 1985, 1987), concluded that the groundwater salinity was derived as a result of interaction of meteoric groundwater with the granite, principally through hydrolysis reactions of plagioclase and biotite.

Methods

Experimental

Hydrothermal experiments were designed to provide qualitative data concerning the nature of the dominant geochemical reactions governing the interaction of meteoric groundwater with granite across the temperature range studied and do not constitute an attempt to quantify mineral dissolution/growth rates or mineral solubilities. Further experimental work to quantify the rates of some of the major geochemical reactions identified are currently in progress.

Experiments were carried out in direct-sampling autoclaves as described by Seyfried et al. (1979) and as utilised by Savage (1986), at 80°, 150° and 250° C for 200, 150 and 100 days, respectively, and at a fluid/rock ratio of 10 (by mass) or 3×10^{-3} cm (by volume/area) falling to ratios of 5 and 1×10^{-3} cm at run completion. An arbitrary pressure of 50 MPa was chosen for all the experiments to prevent the fluid phase from boiling at temperatures in excess of 100° C, and also to aid interpretation of the solution analytical data by a speciation/mass transfer computer program, EQ3/6 (Wolery 1979), which utilised a 50 MPa thermodynamic database. It is believed that a confining pressure of 50 MPa is intermediate between the pressure pertaining during circulation at the Rosemanowes test site and that experienced by natural groundwaters at 2 km depth in the Carnmenellis Granite. Fluid pressures used during circulation tests at Rosemanowes reach 30 MPa (C. Wilkins, personal communication). Pressures relevant to the natural system at 2 km depth would be expected to range from 20 MPa as a hydrostatic component, relating to groundwater in an open fracture network, to 60 MPa for unconnected pore fluids in the granite subjected to lithostatic load pressure. The effect of these different pressures on mineral-fluid reactions is less easy to assess. For such a non-equilibrium system, information is required on the pressure dependence of rate constants. Unfortunately, no such data exist for the temperature-pressure range considered here. However, if the driving force for dissolution is governed by the degree of departure from equilibrium, then pressure effects upon solubilities of minerals may be relevant. Using quartz as an example, the data compilation of Walther and Hèlgeson (1977) indicates that the solubility of quartz at 250° C and 50 MPa is roughly equivalent to that at 265° C and 20 MPa. The increased pressure from 20 to 50 MPa produces an 'apparent' temperature increase of 15° C. Lasaga (1984) quotes an average activation energy for silicate mineral dissolution as 60 kJ mol^{-1} which implies an order of magnitude increase in rate for every 30° C temperature increase. Thus an increase in pressure from 20 to 50 MPa may cause an increase in reaction rates by a factor of 5.

Starting materials were samples of drill chippings taken from a depth of approximately 1800 m from the project borehole designated RH11 at the Camborne HDR site and a sample of water taken from a quarry near to the HDR site which is used as a make-up fluid in the geothermal circulation system, but is also representative of a typical meteoric groundwater of the area. The drill chippings consisted of grains 1–4 mm in diameter whose surface area was 0.325 m^2 g^{-1} as determined by krypton BET. The drill chippings had been washed with deionised water prior to the experiments, but no attempt had been made to remove fine surface debris by ultrasonic or etching techniques. Holdren and Berner (1979) noted that fine, sub-micron debris on feldspar surfaces produced spurious, initial reaction kinetics during dissolution experiments and thus advocated the removal of such particulates by a complex process of etching and washing. However, Moore et al. (1985) have recently questioned the necessity of such procedures where the main aim of experimentations is the characterisation of steady-state fluid chemistry and reaction products, rather than the determination of rate constants. The mineralogy of the chippings is discussed below.

The water from the Trolvis Quarry is a dilute Na–Ca $-HCO_3-Cl$ fluid (Table 1) with a total dissolved solids content less than 120 mg l^{-1}. Nine fluid samples of approximately 10–12 ml in volume were extracted from each experiment, the last sample of which was taken after the autoclave had been allowed to cool to room temperature.

Analytical

(i) *Fluid phase.* On extraction of each sample from the autoclave a 0.5 ml aliquot was used to determine pH and bicarbonate content by glass electrode and titration, respectively. The remaining sample was filtered through a 0.2 μm filter. A 5 ml aliquot of the filtrate was then acidified with 0.1 ml of Aristar grade concentrated hydrochloric acid to stabilise the metal ions in solution and made up to 10 ml with deionised water. This sample then being analysed by inductively coupled plasma (I.C.P) for Na, K, Ca, Mg, Al, Si, B, Fe, Sr, Ba and Li, sulphate was also determined as total sulphur

Table 1. Chemical analysis of water from the Trolvis Quarry ($mg\,l^{-1}$)

pH	7.3
Na	19.4
K	3.4
Ca	9.6
Mg	3.2
Al	0.1
SiO_2	0.2
Cl	31.7
SO_4	19.7
ΣCO_2	15.0
B	0.03
F	0.8
Br	0.155
Fe	0.013
Sr	0.001
Ba	0.011
Li	0.01

which was assumed to be present as sulphate alone. The remaining unacidified portion of the filtrate was then used to determine the halide content: F by ion selective electrode; Cl by colorimetry (Zall et al. 1956), and Br by colorimetry (Fishman and Skougstad 1963) or ion chromatography. The initial starting fluid (Trolvis Quarry water) was analysed in a similar manner to that described above apart from aluminium which was below I.C.P. detection limits ($0.1\,mg\,l^{-1}$) and was determined using the colorimetric method of Sampson and Fleck (1984).

(ii) *Solid phases.* Samples of drill chippings, RH 11/1800 (taken from a depth of 1800 m in borehole RH 11) used in the hydrothermal experiments were characterised by scanning electron microscope (SEM) before and after hydrothermal runs. Rough-fractured granite fragments about 2 cm in diameter taken from cored granite (RH 11/1780) were also mounted on aluminium SEM stubs using conducting carbon cement. These fragments were examined in order to study grain-boundary features. SEM analysis of stub-mounted samples was carried out using secondary electron imaging (standard SEM mode) with a Cambridge Instruments Stereoscan 250 scanning electron microscrope and mineral identification was aided by qualitative chemical analysis obtained from a Link Systems 860 energy-dispersive X-ray microanalyser (EDS) attached to the SEM.

Polished thin sections of RH 11/1780 were also examined both in the SEM using backscattered electron imaging and by standard optical petrographic microscrope. Modal analysis of the core was determined by optical point-counting and checked by studying backscattered electron SEM images.

Quantitative chemical analysis of the major minerals in the granite was carried out by electron microprobe analysis of polished sections of RH 11/1780. Major elements (Na and higher atomic numbers) were measured using a Cambridge Instruments Geoscan Mark II with a Link Systems energy-dispersive microanalyser. F, Cl, Sr, Ba were analysed by wavelength dispersive X-ray microanalysis using a Cambridge Instruments Microscan V electron microprobe. Further wet-chemical analysis of separates of pure muscovite, biotite and tourmaline for Li, B, F and Cl (described later) was also made. These separates were prepared by magnetic separation from drill chippings (RH 11/1800) followed by hand-picking of pure grains.

Trace minerals in the drill chippings were identified by SEM and X-ray powder diffraction photography after concentration by heavy liquid separation in bromoform (after removal of biotite, muscovite and tourmaline by magnetic separation). X-ray powder diffraction photographs were also used to identify hand-picked altered grains after hydrothermal runs. Finely ground samples of granite drill chippings (RH 11/1800) and core (RH 11/1780) were fused with lithium metaborate and dissolved in hydrochloric acid, the resulting solutions were analysed for Si, Al, Fe, Mg, Ca, Na, K, Ti, Mn, Ba and Sr using ICP. Further samples of the aforementioned whole rock and samples of mineral separates from the drill chippings (muscovite, biotite and tourmaline) were fused with Aristar grade sodium carbonate and taken up in Aristar grade nitric acid, insoluble silica being removed by filtration. This sample preparation allowed the elements Li and B to be determined on the whole rock as well as K, Ca, Mg, Mn, Fe, Al, Ba and Sr on the mineral separates, again using ICP. Fluoride in the whole rock sample was determined by two methods. Firstly using a pyrohydrolytic ion-selective electrode technique similar to that used by Clements et al. (1971), and, secondly by analysing the solution from the sodium carbonate fusion with a fluoride ion-selective electrode with standard additions to compensate for matrix effects. Agreement between the two methods was good and the latter method, which was less time consuming, was used to determine the fluoride content of the mineral separates. The solutions produced from the sodium carbonate fusion were also used to determine chloride and bromide. Chloride analysis was performed using the colorimetric method previously described (coupled with standard additions to overcome matrix effects) whereas bromide analyses were performed using the autoanalyser indirect colorimetric method. For all samples the bromide concentration proved to be close to or below the detection limit by this method (0.1 ppm in the solid).

Results

Mineralogy and petrology of RH 11/1780 and RH 11/1800

Whole-rock chemical analyses, and normative and modal mineralogies of samples RH 11/1780 and RH 11/1800 are given in Table 2. CIPW norms have been calculated on the basis that all the Fe is apportioned to magnetite and ilmenite since only total Fe as Fe_2O_3 was determined. RH 11/1780 is a muscovite-biotite adamellite composed dominantly of quartz, K-feldspar and plagioclase with subordinate muscovite, biotite and tourmaline. RH 11/1800 would appear to be similar but contains a greater range and abundance of sulphide minerals which together with willemite (Zn_2SiO_4) and calcite suggest that this drill run may have cut through a mineralised zone of the granite. Furthermore, many of the biotites in RH 11/1800 display partial alteration to chlorite whereas chlorite in RH 11/1780 is only very minor.

The granite is peraluminous as indicated by normative corundum and this is reflected in the actual mineralogy by the presence of muscovite, biotite and andalusite. The rock is generally coarse-grained with the development of porphyritic megacrysts predominantly of K-feldspar but to a lesser extent of quartz also. Patches of finer grained microgranite composed mainly of quartz and plagioclase occur within the groundmass. The textures observed in RH 11/1780 are similar to those described by Stone (1979).

Plagioclase is the only mineral displaying significant variations in composition (Table 3, analyses 1–5). It exhibits subhedral crystals with zonal variation from andesine cores (An_{40}) to albite rims (An_8). Sr varies with Ca content and reaches greatest concentrations in plagioclase cores. Ba was below the detection limits of the microprobe. The cores are commonly altered mainly to sericite (fine muscovite) but some plagioclases show partial replacement of their cores by K-feldspar ("rapakivi" texture). Albite also occurs as exsolution blebs and lamellae within the micro-perthitic K-feldspar and as small subhedral inclusions arranged zonally within K-feldspar megacrysts. Typically this albite has a very low Ca content (Table 3, analysis 6).

Table 2. Chemical, normative and modal analyses of Carnmenellis Granite core, RH11/1780 and drill chippings RH11/1800

	RH11/1780	RH11/1800
Chemical analysis (wt%)		
SiO_2	74.30	73.57
TiO_2	0.13	0.13
Al_2O_3	14.52	14.88
Fe_2O_3 (total)	1.28	1.28
MnO	0.10	0.10
MgO	0.22	0.24
CaO	0.92	0.63
Na_2O	3.51	3.45
K_2O	4.83	4.84
Total	99.71	99.02
	ppm	
B_2O_3	1100	500
Li_2O	700	800
Ba	133	143
Sr	129	72
F	1100	1300
Cl	300	90
Normative mineralogy (wt%)		
Quartz	33.10	33.27
Orthoclase	28.55	28.61
Albite	29.70	29.19
Anorthite	4.56	3.13
Magnetite	1.03	1.03
Ilmenite	0.25	0.25
Enstatite	0.55	0.60
Corundum	1.84	2.82
Total	99.58	98.90
Modal mineralogy (%)		
Quartz	33.6	major
K-feldspar	25.9	major
Plagioclase	30.4	major
Biotite	2.2	subordinate
Muscovite	6.8	subordinate
Tourmaline	1.1	minor-subordinate
	Traces (<1%)	
	Chlorite	Chlorite
	Apatite	Smectite
	Monazite	Apatite
	Zircon	Monazite
	Andalusite	Zircon
	Pyrite	Andalusite
	Fluorite	Willemite
	Pyrite	Pyrite
	Ilmenite	Galena
	Uraninite	Chalcopyrite
	Gypsum/Anhydrite	Sphalerite
	Halite	Molybdenite
	Graphite	Ilmenite
		Rutile
		Magnetite
		Goethite
		Calcite
		Fluorite

K-feldspar occurs interstitially and as large megacrysts; both are micro-perthitic and often contain inclusions of quartz and plagioclase. Typically coarser K-feldspar overprints earlier fabrics and would appear to be replacive, with irregular, cross-cutting grain boundaries. K-feldspar analyses (Table 3, analysis 7) vary little and show up to 5% albite solid-solution (0.6% Na_2O). Ba and Sr were below microprobe detection limits.

Biotite and muscovite are closely associated, with muscovite either replacing biotite laths along cleavages or forming irregular syntaxial overgrowths on biotite. Only very minor alteration of biotite to chlorite was evident in RH11/1780 but chloritization is more common in RH11/1800. Clots of biotite were occasionally seen and are associated with minor andalusite and more rarely carbonaceous or graphitic material. These clots may represent partly resorbed xenolithic material. Muscovite often exhibits fibroradiate growths of a calcium aluminosilicate mineral (D. Goossens, personal communication) developed along cleavages within the crystals (Fig. 2a). By analogy with alterations observed in fractures from borehole material from the Rosemanowes Quarry, it is inferred that this mineral is laumontite (Ca-zeolite). Both micas contain significant amounts of Li, Mg and F (Table 3, analyses 8–9) but Cl was only detected by microprobe in biotite. Wet chemical determinations of F and Cl from mineral separates in RH11/1800 confirm the microprobe data. Sericite from altered plagioclase differs in composition from coarse muscovite, being deficient in Mg, Ti and Fe (Table 3, analysis 10).

Tourmaline occurs as optically continuous networks within the groundmass and may show slight replacement of feldspars. It is a schorl variety with up to 3% MgO and 0.5% F (Table 3, analysis 11). Tourmaline is the only apparent B phase.

Ilmenite, monazite, apatite, zircon and uraninite occur in trace amounts mostly, but not exclusively, in biotite as inclusions. Their distribution has been studied in detail by Jefferies (1984). Fluorite is a common trace constituent, concentrated along grain boundaries of mica (Fig. 2b). Fluoride is a constituent of both biotite and muscovite, so the association of fluorite with mica is believed to indicate an episode of mica dissolution during water-rock reaction within the granite. Similarly, thin films of a phase(s) rich in Na, Ca, Cl and S (by EDS), also occur along grain boundaries within the core material (Fig. 2c).

Qualitative SEM X-ray analyses of these grain boundary phases were confirmed by analyses of fluids produced by washing known weights of crushed core material and chippings by deionised water. Although the chippings contain negligible amounts of readily-soluble salts (suggesting their loss by flushing with water during drilling), the core contains appreciable amounts of what appears to be $CaSO_4$, together with NaCl, KCl, Na_2SO_4 and K_2SO_4. The presence of these grain-boundary phases would account for the higher Ca, Na and Cl contents of the core as compared to the drill chippings (Table 2). It is envisaged that these readily soluble salts would have been present at depth in situ in the granite as a saline pore-fluid, and have precipitated as a result of the drying of the drill core after extraction from the well bore. The degree of salinity of this inferred pore-fluid may be calculated by using the chemical analysis of the core washing and the porosity of the granite. If a conservative figure of 0.5% is chosen as a value for in situ

Table 3. Electron microprobe analysis of major minerals from RH11/1780

	1	2	3	4	5	6	7	8	9	10	11
SiO_2	57.35	62.02	64.71	65.83	65.80	68.69	64.45 (±0.37)	36.18 (±0.53)	46.12 (±0.28)	46.10 (±0.37)	35.52 (±0.31)
TiO_2								2.28 (±0.34)	0.45 (±0.13)		0.59 (±0.31)
B_2O_3	n.d.	n.d.	n.d.	n.d.	n.d.	n.d.	n.d.	0.01	0.02	n.d.	9.92
Al_2O_3	26.79	24.19	22.79	21.74	21.23	19.16	18.31 (±0.14)	21.26 (±0.34)	33.48 (±0.55)	37.47 (±0.16)	34.09 (0.40)
FeO								21.71 (±0.61)	2.15 (±0.42)		10.44 (±0.50)
MnO								0.54 (±0.09)			
MgO								3.07 (±0.11)	0.92 (±0.14)		2.94 (±0.12)
CaO	8.92	5.10	3.22	2.20	1.84	0.11					0.20 (±0.04)
SrO	0.13	0.08	0.05	0.04	0.04	n.d.					
BaO						n.d.					
Li_2O	n.d.	n.d.	n.d.	n.d.	n.d.	n.d.	n.d.	1.05	0.30	n.d.	0.04
Na_2O	6.49	8.59	9.93	10.13	10.57	11.50	0.62 (±0.05)	0.27 (±0.15)	0.75 (±0.11)	0.30 (±0.12)	2.01 (±0.10)
K_2O	0.22	0.26	0.19	0.33	0.43	0.20	16.55 (±0.23)	9.66 (±0.18)	10.35 (±0.21)	11.25 (±0.21)	
F	n.d.	n.d.	n.d.	n.d.	n.d.	n.d.	n.d.	1.10 (±0.21)	0.81 (±0.09)	n.d.	0.58 (±0.12)
Cl	n.d.	n.d.	n.d.	n.d.	n.d.	n.d.	n.d.	0.10 (±0.02)	0.004	n.d.	0.001
	99.90	100.24	100.59	100.27	99.91	100.46	99.93	97.23	95.35	95.16	96.33
O=F								0.49	0.34		0.24
Total	99.90	100.24	100.59	100.27	99.91	100.46	99.93	96.74	95.01	95.16	96.09
Si	10.302	10.976	11.351	11.542	11.591	11.941	11.960	5.416	6.906	5.398	5.915
Ti								0.257	0.051		0.074
B								0.002	0.005		2.850
Al	5.673	5.047	4.651	4.494	4.409	4.091	4.006	3.754	5.911	6.713	6.692
Fe								2.719	0.269		1.454
Mn								0.068			
Mg								0.685	0.205		0.729
Ca	1.717	0.967	0.605	0.413	0.347	0.021					0.036
Sr	0.014	0.007	0.005	0.004	0.004						
Ba											
Li								0.632	0.180		
Na	2.260	2.948	3.377	3.443	3.610	3.876	0.223	0.079	0.218	0.088	0.648
K	0.050	0.060	0.042	0.074	0.097	0.044	3.919	1.845	1.978	2.181	
F								0.521	0.383		0.305
Cl								0.025	0.001		
O	32.000	32.000	32.000	32.000	32.000	32.000	32.000	22.000	22.000	22.000	29.000

1–5 Plagioclase core-rim; *6* Albite exsolution in K-feldspar; *7* K-feldspar (mean 5 analyses); *8* Biotite (mean 10 analyses except F, Cl mean 9 analyses and B_2O_3, Li_2O determined by wet chemistry on two samples from RH11/1800); *9* Muscovite (mean 10 analyses except F mean 6 analyses and Cl, B_2O_3 and Li_2O determined by wet chemistry on two samples from RH11/1800); *10* Sericite (mean 3 analyses); *11* Tourmaline (mean 7 analyses except Cl, B_2O_3 and Li_2O determined by wet chemistry on one sample from RH11/1780). *n.d.* not determined

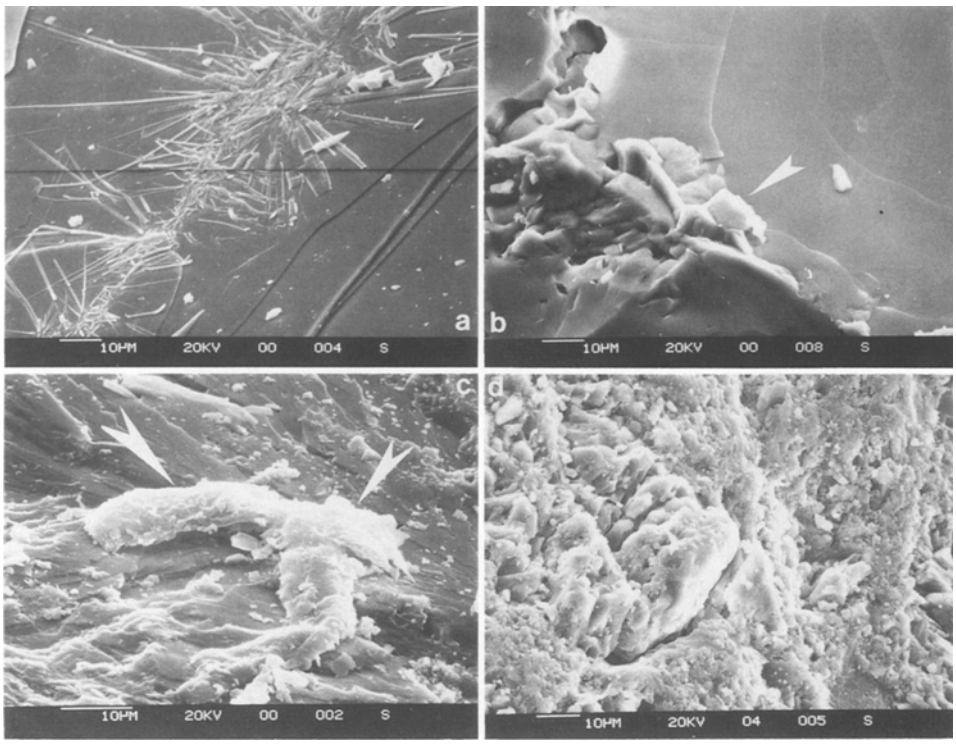

Fig 2a–d. SEM photomicrographs of Carnmenellis Granite prior to experimentation. **a** Fibrous calcium aluminosilicate (laumontite?) upon a substrate of muscovite (RH11/1780). **b** Fluorite crystals (*arrowed*) nucleating at a quartz-biotite grain boundary (RH11/1780). **c** Crystals of $CaSO_4$-NaCl coating aluminosilicates (RH11/1780). **d** A 'fresh' plagioclase surface (RH11/1800)

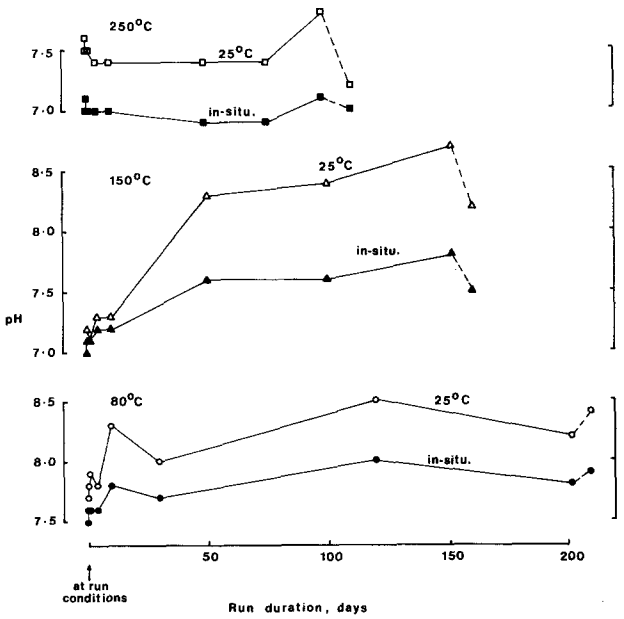

Fig. 3. pH of experimental fluids versus time. *Open symbols* indicate pH as measured at 25° C, whereas *filled symbols* show in-situ pH as calculated from measured pH using the computer program EQ3/6. The *dashed tie line* links the final quenched sample to the rest of the data. *Filled circles*, *triangles* and *squares* refer to the 80°, 150° and 250° C experiments respectively

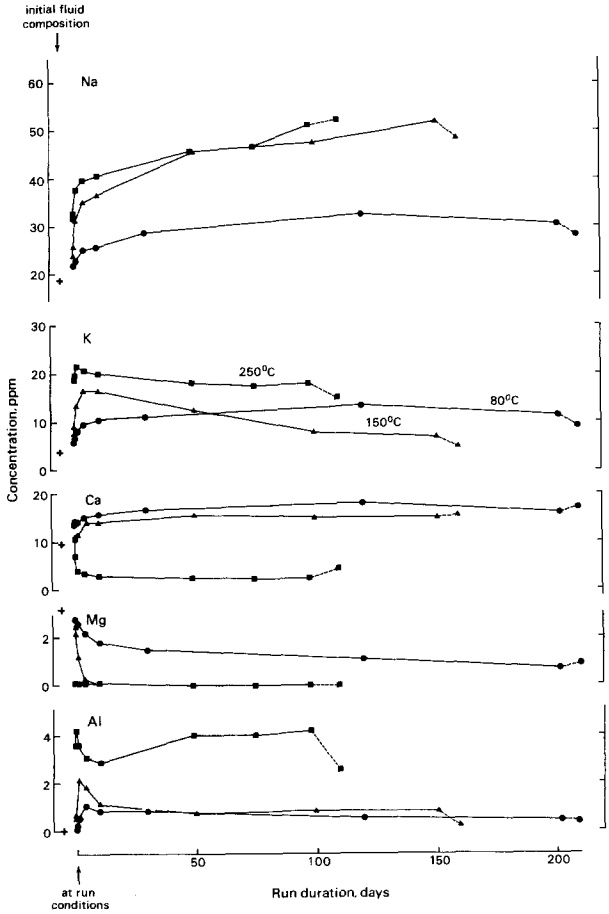

Fig. 4. Concentrations of Na, K, Ca, Mg and Al (in ppm) in experimental fluids versus time. The *dashed tie line* links the final quenched sample to the rest of the data. *Filled circles*, *triangles* and *squares* refer to the 80°, 150° and 250° C experiments respectively

porosity, then this implies the presence of a pore fluid with a salinity several times that of seawater in the granite prior to drilling, if all the pores are saturated with fluid.

SEM examination of drill cuttings and core fragments show that many of the mineral grains exhibit evidence of pronounced episodic 'natural' water-rock reactions as a result of hydrothermal circulation after the emplacement of the granite (Fig. 2d).

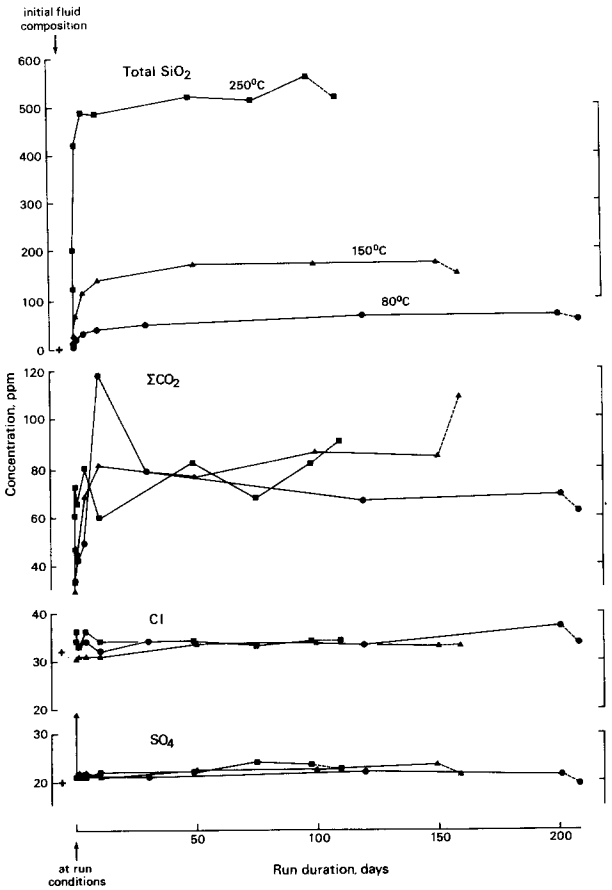

Fig. 5. Concentrations of SiO_2, CO_2, Cl and SO_4 (in ppm) in experimental fluids versus time. The *dashed tie line* links the final quenched sample to the rest of the data. *Filled circles*, *triangles* and *squares* refer to the 80°, 150° and 250° C experiments respectively

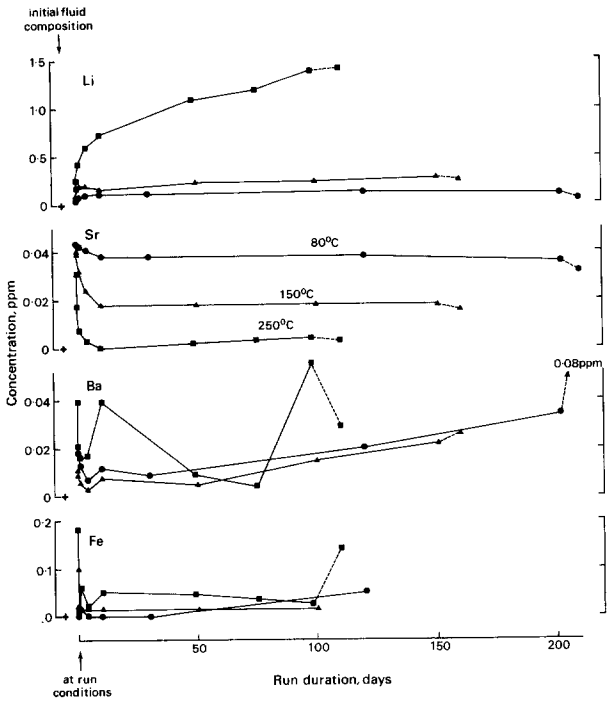

Fig. 6. Concentrations of Li, Sr, Ba and Fe (in ppm) in experimental fluids versus time. The *dashed tie line* links the final quenched sample to the rest of the data. *Filled circles*, *triangles* and *squares* refer to the 80°, 150° and 250° C experiments respectively

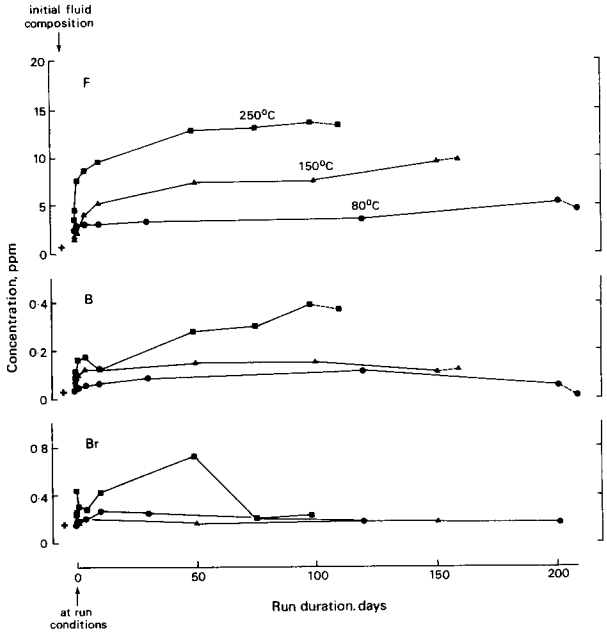

Fig. 7. Concentrations of F, B, and Br (in ppm) in experimental fluids versus time. The *dashed tie line* links the final quenched sample to the rest of the data. Bromide data were acquired by ion chromatography except for samples from the 250° C experiment prior to 50 days duration which were analysed by a colorimetric method. *Filled circles*, *triangles* and *squares* refer to the 80°, 150° and 250° C experiments respectively

Fluids from the hydrothermal experiments

Analytical data from the experiments are illustrated graphically in Figs. 3–7 and will not be described in detail here. Tabulations of analytical data from the experiments may be obtained from the authors. In general, the geochemical interactions are dominated by the development of time-invariant or time-decreasing concentrations. These characteristics are developed most rapidly with increasing temperature, so that concentration maxima appear within 5 days at 250° C, increasing to roughly 30–50 days at 150° C and 100–200 days at 80° C. Only the behaviour of Na (at 150° and 250° C), Li (at 250° C), Ba (at 80° and 150° C), F (at all temperatures) and B (at 250° C) appear dominated by 'forward' dissolution reactions of primary phases. The development of steady-state or decreasing concentrations is interpreted as being due to the nucleation and growth of more stable secondary solid phases from the primary minerals. A number of components (e.g., Na, K, SiO_2) show enhanced release to the fluid during the initial five days of the experiments which may be due to a removal of fine particulates and high surface energy features on the mineral grains (e.g., Berner and Holdren 1979). Data for pH (Fig. 3) are somewhat irregular which probably results from CO_2 loss prior to, and during, pH measurement. The evolution of pH with time varies with temperature, but remains alkaline throughout, in the range pH 7–9. In situ pH values were calculated using the computer program EQ3/6, in the manner described by Savage (1986). These in situ values broadly follow those as measured at 25° C, but are approximately 0.5 pH units lower. This decrease of pH at higher temperatures may be accounted for by the dissociation con-

stant of water increasing with temperature so that neutral pH at 80°, 150° and 250° C is 6.3, 5.6 and 5.5, respectively (Helgeson 1969).

Solids from the hydrothermal experiments

The observable effects of mineral dissolution and growth increased progressively with temperature. In all cases the most obvious effect seen in the solid phase as a result of hydrothermal reaction was the dissolution of loose, adhering, fine, particulate debris (produced during drilling) from the grain surfaces. This debris has a mineralogy similar to that of the bulk sample but is generally less than 5 μm (Fig. 8a). After completion of the 250° C run only the coarsest particles remained on grain surfaces (Fig. 8b). No effect other than the loss of fine particulates was observed in the residue from the 80° C experiment.

At 250° C quartz, K-feldspar, plagioclase and tourmaline show varying degrees of dissolution but biotite and muscovite appear to have reacted to only a minor extent. Both K-feldspar and plagioclase show the greatest degree of dissolution with relatively extensive etching and pitting picking out cleavage directions (Fig. 8c). The features displayed are similar to those described by Berner and Holdren (1979) in weathered feldspar. However, this etching is complicated by the fact that much of the feldspar present initially in RH11/1800 has already suffered corrosion and many grains are coated or encrusted with goethite. It was therefore often impossible to distinguish corrosion as a result of experimentation from the original corrosion features. It was only in the 250° C experiment that the corrosion was so extensive as to be clearly caused by the experimental conditions, although minor consistent corrosion also suggested that the same processes were occurring at 150° C. Quartz and tourmaline only showed signs of reaction in the 250° C residue. They displayed slight pitting of mineral surfaces and rounding of sharp fractured edges (Fig. 8). In quartz grains fluid inclusions had been opened up and etching commonly picked out such lines of weakness (Fig. 8d). The sulphide minerals commonly present in the starting material were largely absent or obscured from the residue of the experiments; only galena was observed directly in the 250° C residue and exhibited corrosion and rounding of its cubic crystals (Fig. 8e).

Smectite was identified as a reaction product from both the 150° C and 250° C experiments but was most extensively developed in the latter where it was identified by XRD in hand-picked grains. It is the most abundant secondary phase, present on all mineral surfaces but it seems to be particularly well developed on highly altered, porous grains presumed to be previously altered feldspar (Fig. 8f). This smectite has a typically 'rosetted' habit and encrusts grain surfaces. X-ray spectra of the smectite show it to be composed chiefly of Si, Al, Ca, Fe, K with some Mg and Na. Where it is associated with aggregates of galena, it may also contain significant Zn. Elsewhere the smectite is less well developed and is commonly only present as fine wispy growths on grain surfaces of quartz, tourmaline or mica (Fig. 8g). These fine precipitates are often too small to be identified by EDS spectra on the SEM and had been previously attributed to amorphous silica (Savage et al. 1985) but a reexamination suggests they are "proto-smectite" growths. A well-crystallised Ca, Al, Si phase with cubic or pseudo-cubic symmetry occurs sparsely on all mineral phases at 250° C, but like smectite is particularly abundant on previously altered feldspar (Fig. 8h. This phase was tentatively identified by Savage et al. (1985) as laumontite but its symmetry suggests that wairakite is the most likely mineral. Other minor secondary products identified as fine precipitates in the experiments are calcite (150° C and 250° C) and calcium sulphate (anhydrite or gypsum, 250° C only). These minerals are generally poorly crystallized and occur sparsely on all minerals as highly corroded grains. This corrosion is inferred to have taken place during the quench process.

These reaction products are similar to those described by Charles (1978), Charles and Bayhurst (1983), Bourg et al. (1985) and Savage (1986). Charles (1978) observed an order of reactivity of quartz > microcline > plagioclase > mafic minerals during reaction of granodiorite with distilled water at 300° C and 35 MPa in a flow-through autoclave system. The quartz-undersaturated nature of the circulating fluid encouraged the growth of secondary zeolites (phillipsite and thomsonite), and an iron rich clay (vermiculite) was also observed. Charles and Bayhurst (1983) noted the secondary precipitation of Ca-montmorillonite at 72° C and 119° C, a zeolite (stilbite or heulandite) at 161° C, and another zeolite (thomsonite) at 209°–310° C, during reaction of a biotite granodiorite with distilled water in a flow through autoclave system. These authors, also noted strong etching of quartz at temperatures greater than 161° C, congruent dissolution of microcline and recrystallisation of plagioclase, whereas biotite appeared inert. Bourg et al. (1985) did not make any direct observations concerning secondary mineral formation during reaction of granite with distilled water at 100° C, but inferred the possible precipitation of numerous aluminosilicates from saturation index calculations. Savage (1986) noted the occurrence of a smectite clay as the most important secondary product of granite-water reaction at 100° C.

Chemical exchange during water-rock reaction

A knowledge of the chemical composition of experimental fluids, the minerals in the granite, and solids precipitated during the course of the experiments, enables the construction of a mass balance in order to identify chemical reactions important in determining the type and pattern of water-rock interaction. The following is an attempt to summarise the evidence of 'sources' (reactant solids or fluid)

Fig. 8a–h. SEM photomicrographs of mineral grains from RH11/1800 prior to, and after reaction at 250° C. **a** A tourmaline grain prior to experimentation showing the distribution of surface particulates. **b** A tourmaline grain after reaction showing near-complete removal of surface particulates, together with distinct surface etch-pitting. **c** A plagioclase grain from the 250° C experiment revealing pronounced etching along cleavages and removal of fine surface debris. **d** A quartz grain from the 250° C experiment exhibiting etched fluid inclusion trails. **e** A cubic galena grain showing etch features and a mat of Zn-rich smectite developed after reaction. **f** Rosetted aggregates of smectite covering a primary aluminosilicate after reaction. **g** Flakes of smectite developed upon quartz after reaction. **h** Angular crystals of Ca-aluminosilicate (wairakite?) and a network of smectite developed upon plagioclase after reaction

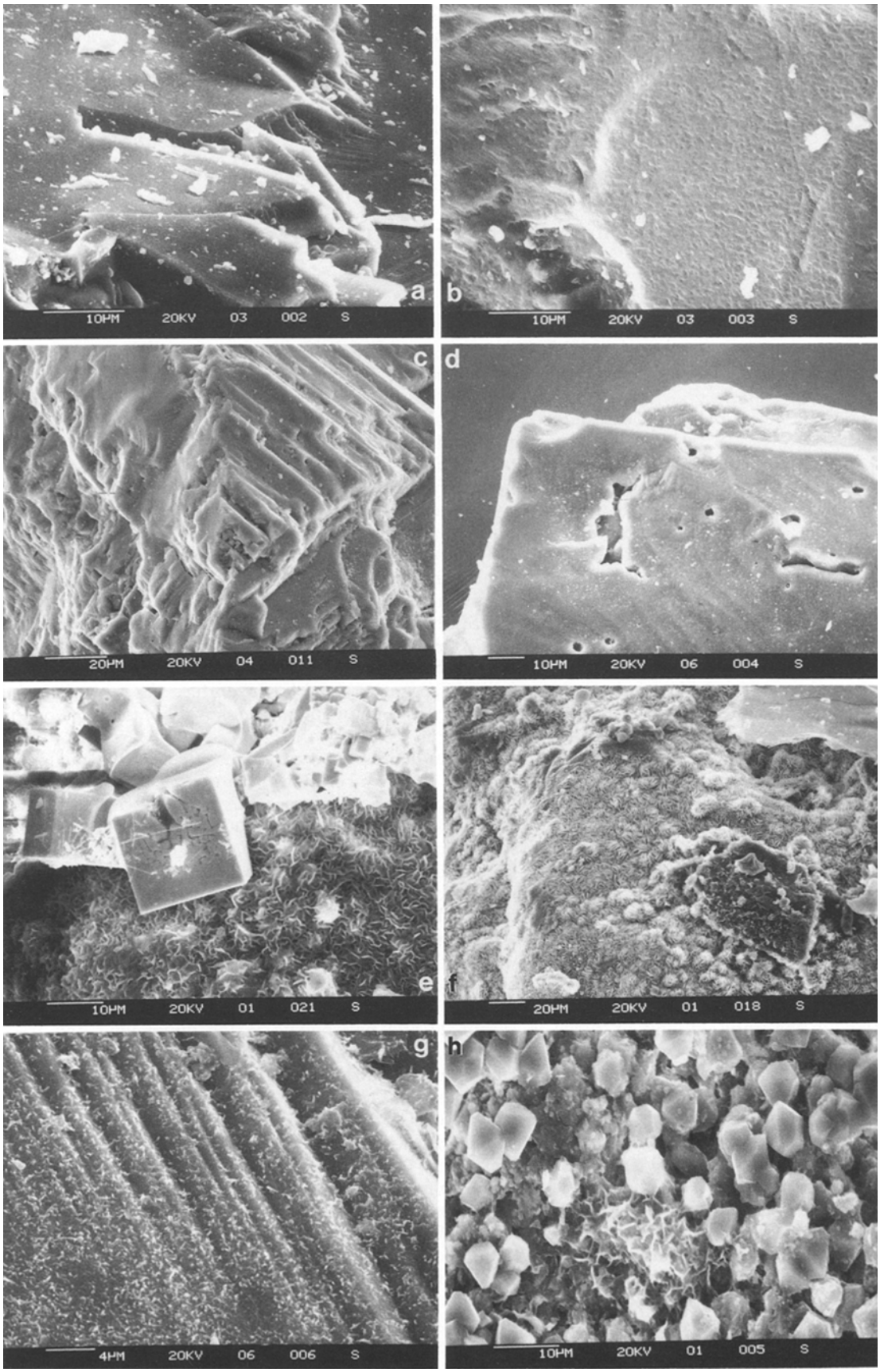
a
10μM 20KV 03 002 S
b
10μM 20KV 03 003 S
c
20μM 20KV 04 011 S
d
10μM 20KV 06 004 S
e
10μM 20KV 01 021 S
f
20μM 20KV 01 018 S
g
4μM 20KV 06 006 S
h
10μM 20KV 01 005 S

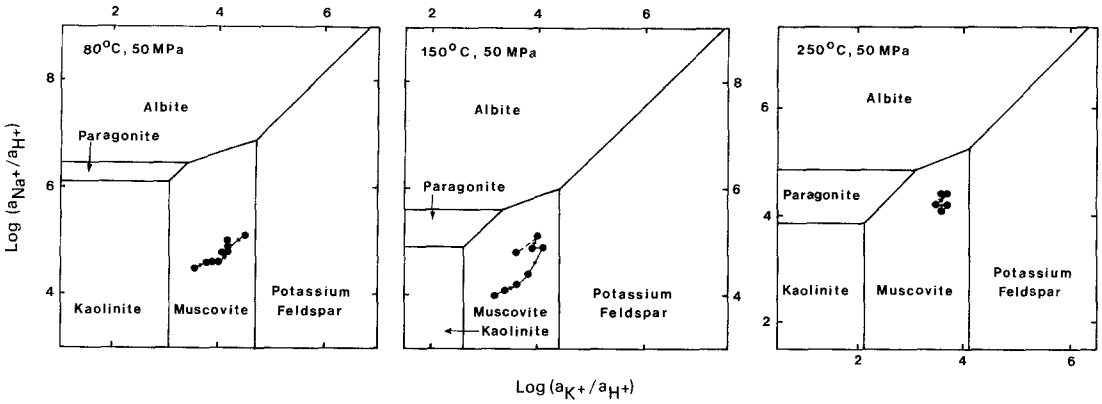

Fig. 9. Fluid phase Na/H and K/H activity ratios plotted on a logarithmic activity diagram for the system $K_2O-Na_2O-Al_2O_3-HCl-H_2O$. Silica activity is defined by quartz solubility. Mineral stability-fields were constructed from the data of Helgeson et al. (1978). *Arrows* indicate increasing time. *Dotted tie lines* link quench fluids to the rest of the data

and 'sinks' (product solids or fluid) for each element of interest during each experiment.

The major mineral source of sodium in the granite is plagioclase. Loss of sodium from the fluid to a secondary smectite clay was observed at 150° and 250° C. Roughly 85% of the total potassium in the granite is concentrated in potassium feldspar, with muscovite accounting for 12%. Biotite is responsible for the remainder. The only secondary potassium bearing mineral phase identified was a smectite clay. Consideration of an equilibrium activity diagram for Na and K (Fig. 9) shows that the experimental fluids were undersaturated with both Na and K-feldspars and saturated with muscovite. Unfortunately no suitable thermodynamic data for smectite clays are available at these elevated temperatures, although it is anticipated that stability-fields for Na- and K-smectites would be between the paragonite-kaolinite and muscovite-kaolinite fields respectively (Aagaard and Helgeson 1983; Giggenbach 1985). Consequently, it may be envisaged that the clustering of experimental data points observed in Fig. 9 lie within the hypothetical stability field of K-smectite. This would concur with the evidence from the retrieved solids which implies marked dissolution of plagioclase, minor dissolution of K-feldspar and muscovite and the precipitation of a potassium dominated smectite clay. Figure 9 also emphasises the instability of kaolinite in the experimental fluids.

Calcium is almost wholly concentrated in plagioclase, with minor concentrations in the trace amounts of calcite and fluorite in the chippings. SEM observations of secondary phases were partially confirmed by information about mineral saturation states as given by the computer program EQ3/6 which indicated saturation of calcite throughout each experiment, saturation of laumontite during the 80° C run and saturation of anhydrite during the 250° C run. In addition, saturation of the fluid with respect to fluorite occurred at each temperature. Laumontite stability at each temperature was investigated further by the construction of a pH-potassium activity diagram (Fig. 10, in part after Crossey et al. 1984). A stability field for K-smectite was omitted from Fig. 10 for the same reasons given for Fig. 9. It is envisaged that the smectite stability range would lie between laumontite, kaolinite and muscovite, so that smectite is apparently stable at 80° C and laumontite-smectite at 150° C and at 250° C. Laumontite partially dehydrates at approximately 260° C (at 50 MPa) so that wairakite becomes the stable Ca-zeolite above this temperature (Liou 1971). The tentative identification of wairakite in the 250° C run products indicates that this may be metastable growth of wairakite, or that the laumontite-wairakite reaction boundary may occur at a lower temperature than suggested by Liou's (1971) data. It is noteworthy that the experimental fluids are too alkaline for the growth of kaolinite.

Although the Mg in the initial system is almost entirely in the granite (it is about 50 greater in the granite than in the fluid), it is difficult to assess dissolution of the principal Mg-bearing minerals (biotite and tourmaline) because of the net loss of Mg from the fluid during the experiments. However, Savage et al. (1986) noted that the solution phase in the experiments at each temperature was supersaturated with respect to phlogopite which may have inhibited biotite dissolution.

The aluminium content of the experimental fluids was buffered at all temperatures by progressive dissolution and growth of primary and secondary mineral phases, respectively, its concentration in solution being directly related to temperature.

Solubility calculations indicate that silica concentrations in solution during the experiments matched that of quartz, despite dissolution of all the primary silicates contributing silica to solution.

Bicarbonate concentrations in solution were roughly constant with time, bearing in mind analytical problems outlined above. Sources of ΣCO_2 included dissolved CO_2, carbonate and bicarbonate in the initial fluid and trace amounts of calcite contained in the drill chippings. The precipitation of calcite during the experiments apparently served to maintain the ΣCO_2 content of the fluid at a constant level. The minor release of chloride during the experiments reflects the relatively low content of this element in the rock (90 mg kg^{-1}, Table 2). The chloride present as grain boundary salts observed with the SEM would not have been present in the starting materials due to washing of the chippings during drilling. Biotite, muscovite and tourmaline account for 24, 3 and 2% of the total chloride respectively, with fluid inclusions presumably accounting for the remainder. Release of sulphate during the experiments was limited to oxidation of trace sulphides present within the chippings.

Inventory calculations show that biotite accounts for roughly 30% of the total rock lithium content, with muscovite accounting for 27% and tourmaline 6%. The remainder is assumed to be spread across a number of other phases.

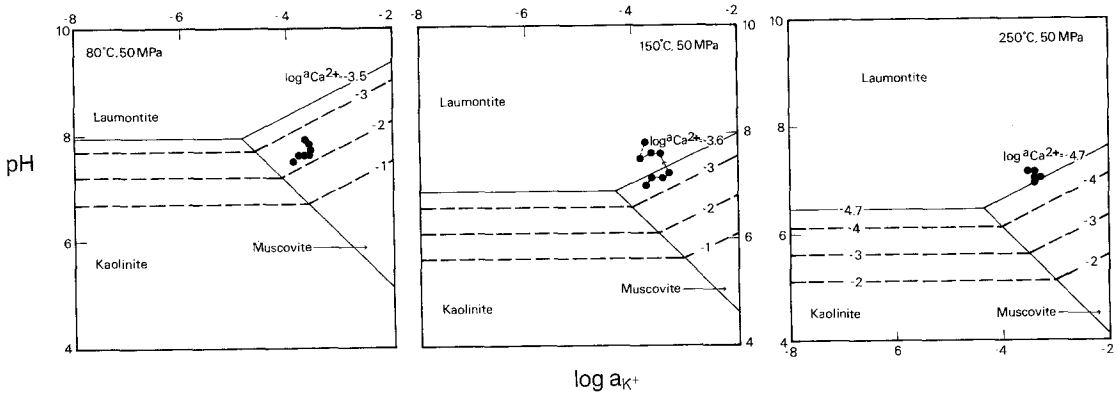

Fig. 10. Fluid phase pH versus logarithmic K^+ activity for the system $CaO-K_2O-Al_2O_3-SiO_2-HCl-H_2O$. Silica activity is defined by quartz solubility. *Dashed lines* indicate isopleths of logarithmic calcium activity. *Solid boundaries* between laumontite-kaolinite and laumontite-muscovite were constructed using steady-state Ca activities measured in the experiments. Mineral stability fields were constructed from the data of Helgeson et al. (1978). *Arrows* indicate increasing time. *Dotted tie lines* link quench fluids to the rest of the data

This relative order of Li content, together with absolute concentrations compares favourably with a survey of the Li content of minerals from Cornish granites undertaken by Wilson and Long (1983) using an ion microprobe analytical method. Fluid phase data at 80° and 150° C suggest the importance of precipitation or sorption of secondary solid(s) in limiting Li concentration in solution. Although data at 250° C do not unequivocally indicate lithium release without secondary precipitation/sorption, hypotheses concerning preferential mineral dissolution may be examined in more detail. From Table 3, it may be calculated that if muscovite dissolution alone were to account for the final lithium concentration in solution at 250° C (1.39 mg l^{-1}), then congruent dissolution of this phase would also account for 7 mg l^{-1} fluoride and 0.03 mg l^{-1} chloride in solution. Similarly, biotite dissolution alone would contribute 2.5 mg l^{-1} fluoride together with 0.3 mg l^{-1} chloride. Parallel calculations for tourmaline indicate a solution content for fluoride and chloride of 0.2 mg l^{-1} and 1 mg l^{-1}, respectively. However, this amount of tourmaline dissolution would also produce 230 mg l^{-1} B in solution, whereas 0.4 mg l^{-1} of B was actually measured in solution. Therefore, muscovite and/or biotite dissolution would be compatible with the data for Li, F and Cl.

Strontium was concentrated almost wholly in plagioclase in the starting materials. Sr was not observed in qualitative X-ray spectra of fluorites examined by SEM. The temperature dependent steady-state concentrations observed in the experimental fluids indicates that Sr was preferentially partitioned into a secondary solid, probably calcite. Ba was probably concentrated in K-feldspar (substituting for K ions) in the starting materials. Fluid data for Ba suggest initial release, then a precipitation sequence, followed by an increase until run termination. Possible secondary solids are barium carbonate or sulphate. Iron was present in the starting solids in a number of phases, namely biotite, tourmaline, pyrite, magnetite and ilmenite. Fe concentrations in the fluid were roughly constant during the experiments. The secondary smectite contained a proportion of Fe, suggesting a parallel release of Fe from an initial solid.

Fluorine was contained in biotite, muscovite, tourmaline and fluorite. In terms of an inventory calculated from the mineral chemical and modal analyses, it may be seen that muscovite accounts for 40% of the total fluoride, biotite 17% and tourmaline 4%. This implies approximately 40% of the total was fluorite (observed as trace grains in the core and chippings). In terms of minerals contributing fluoride to the fluid phase, a number of limiting assumptions may be made, using the data from the 250° C experiment. As stated above, if muscovite contributed all the lithium in solution, it would also provide roughly 50% of the total fluoride in solution. Dissolution of biotite and/or tourmaline could not significantly boost the fluoride content of the solution without also altering the Li content. Fluorite must contribute at least 50% of the total fluoride seen in solution.

Inventory calculations for B show that all the whole rock content of this element may be accounted for in tourmaline. The presence of boron in solution should, therefore, be a sensitive indicator of tourmaline dissolution. Data at 80° C and 150° C are complicated by removal of boron by precipitation of secondary solids or sorption onto mineral phases. Although some precipitation of B at 250° C cannot be ruled out, data from this experiment may be used to calculate the contributions made by tourmaline to the fluid concentrations of Li, F and Cl (assuming stoichiometric dissolution). The final B concentration at this temperature was 0.39 mg l^{-1}. Assuming stoichiometric dissolution, tourmaline would therefore also add 0.002 mg l^{-1} of Li, 0.05 mg l^{-1} of F and 0.002 mg l^{-1} of Cl. The minor amounts of tourmaline dissolution observed would have had a negligible effect upon the concentration of Li, F and Cl in the solutions and may be ignored as a source for these consituents. However, there would be a concomitant release of over 1 mg l^{-1} of Fe in solution, which is roughly 40 times that actually measured, and may provide a source of Fe for incorporation into smectite. The relative inertness of tourmaline as suggested by the fluid chemical data is also corroborated by the morphological evidence described above ('solid phases'). Tourmaline revealed minor dissolution features only at 250° C, which were much less pronounced than those observed on plagioclase and potassium feldspar.

The source of bromide in the starting solids has not been determined, although it has been inferred by Edmunds

et al. (1985) that bromide substitutes for chloride in the biotite structure of the Carnmenellis Granite.

Discussion

Mineral-fluid reactions

The above discussion concerning the origin and fate of chemical components during water-rock reaction enables some generalised reactions to be constructed at each experimental temperature. In view of the non-equilibrium nature of the interactions, these reactions should be regarded as schematic, but serve to constrain the overall exchange between minerals and fluid. In addition, because of the dilute nature of the starting fluid, it is probable that all starting solids reacted to a certain degree. The following discussion concentrates on those mineral phases and chemical components which appear to have dominated the chemistry of the fluid and the nature of secondary solids. Because of the complexity of writing balanced chemical reactions involving trace components, these have been omitted but the constraints placed upon major element exchange by trace components will be noted where necessary.

At 250° C, fluid, mineralogical and theoretical evidence suggest that major dissolving phases were plagioclase and K-feldspar. Fluid data for Li and B also indicate progressive dissolution of muscovite and/or biotite and tourmaline. Secondary solids were laumontite/wairakite, a K−Mg−Na smectite clay, calcite, anhydrite and amorphous silica. Anhydrite was precipitated in trace amounts which served to limit concentrations of SO_4 in solution. The relatively minor amounts of anhydrite growth during the experiment is confirmed by the lack of an increase in SO_4 concentration in solution at the termination of the experiment which would be caused by the retrograde solubility of anhydrite. However, Savage et al. (1985) noted that anhydrite grains were skeletal, suggesting dissolution during cooling of the autoclave. Saturation index calculations on the fluid phase also indicate equilibrium of the fluid with fluorite. Since fluorite was a minor constituent of the initial drill chippings, it has been omitted from the reaction below. The interaction at 250° C is best described by the following equation:

$$\underset{\text{plagioclase (andesine)}}{15\,Na_{0.66}Ca_{0.33}Al_{1.33}Si_{2.66}O_8} + \underset{\text{K-feldspar}}{KAlSi_3O_8} + \underbrace{0.4\,Mg^{2+} + CO_2 + SO_4^{2-} + 0.5\,Ca^{2+} + 10\,H^+}_{\text{from fluid}} + 22\,H_2O \longrightarrow$$

$$\underset{\text{wairakite}}{3.5\,CaAl_2Si_4O_{12}\cdot 2\,H_2O} + \underset{\text{smectite}}{2\,K_{0.5}Mg_{0.2}Na_{0.1}Al_7Si_{11}O_{30}(OH)_6} + \underset{\text{calcite}}{CaCO_3} + \underset{\text{anhydrite}}{CaSO_4} + 7\,H_4SiO_4 + 9.8\,Na^+ \quad (1)$$

Strong zoning of plagioclase feldspar and the absence of a quantitative chemical analysis of the secondary smectite preclude firm conclusions concerning the stoichiometry of the reaction, but reaction (1) serves to illustrate: the loss of Mg, Ca, and protons from the initial fluid; the conservation of Al and K; the release of Na to the fluid; and the precipitation of wairakite, calcite, anhydrite, smectite and silica during reaction.

At 150° C, major dissolving mineral phases were plagioclase and K-feldspar, with minor contributions from muscovite and/or biotite and tourmaline. Secondary solids positively identified were a K−Mg−Na smectite clay and calcite. Laumontite growth may have occurred at this temperature, as suggested by activity calculations, but was undetected by SEM/XRD. A reaction compatible with conservation of Ca and Al, yet showing net release of Na and consumption of Mg and protons would be:

$$\underset{\text{plagioclase (andesine)}}{16.5\,Na_{0.66}Ca_{0.33}Al_{1.33}Si_{2.66}O_8} + \underset{\text{K-feldspar}}{KAlSl_3O_8} + \underbrace{0.5\,K^+ + 0.2\,Mg^{2+} + 4.5\,CO_2 + 9.8\,H^+}_{\text{from fluid}} + 28.1\,H_2O \longrightarrow$$

$$\underset{\text{laumontite}}{CaAl_2Si_4O_{12}\cdot 4\,H_2O} + 3\,\underset{\text{smectite}}{K_{0.5}Mg_{0.2}Na_{0.1}Al_7Si_{11}O_{30}(OH)_6} + \underset{\text{calcite}}{4.5\,CaCO_3} + 10.7\,Na^+ + 10\,H_4SiO_4 \quad (2)$$

Decreasing concentrations of K in the fluid during the 150° C experiment is indicated by the presence of K^+ as a reactant in reaction (2). The composition of reactant plagioclase and product smectite is schematically represented in reaction (2) as being identical to that presented in reaction (1) No quantitative analytical data are available for the secondary smectite. Although the overall analysed composition of plagioclase is that represented in reactions (1) and (2), it may be that different compositional zones in plagioclase may have reacted differently at different temperatures. At 80° C, Na, as well as Ca and Al, was conserved in the fluid phase. Major reactant phases were similar to the 250° C and 150° C experiments, whereas product solids are inferred from saturation index calculations to be smectite and calcite. Due to the stoichiometry of the feldspar – smectite reaction the absence of a peralkaline product such as laumontite necessitates either the involvement of an aluminosilicate phase and quartz as reactants or considerable sorption of Na^+ on solid phases. Aluminosilicates available for reaction consisted of trace amounts of andalusite. The stoichiometry of the plagioclase + K-feldspar + quartz + aluminosilicate → smectite + calcite reaction is such that the aluminosilicate/plagioclase molar ratio is roughly 4. Clearly, with only trace amounts of andalusite available for reaction, this mechanism could not contribute significantly to the mass balance. In the absence of any identifiable peralkaline aluminosilicates in the reaction products, sorption of Na^+ on solid phases is the only means by which Na could be conserved in this reaction. Consequently, the following reaction is relevant:

$$\underset{\text{plagioclase (andesine)}}{15\,Na_{0.66}Ca_{0.33}Al_{1.33}Si_{2.66}O_8} + \underset{\text{K-feldspar}}{KAlSi_3O_8} + \underbrace{0.2\,Mg^{2+} + 0.5\,K^+ + 5\,CO_2 + 8.8\,H^+}_{\text{from fluid}} + 24.6\,H_2O \longrightarrow$$

$$\underset{\text{smectite}}{3\,K_{0.5}Mg_{0.2}Na_{0.1}Al_7Si_{11}O_{30}(OH)_6} + \underset{\text{calcite}}{5\,CaCO_3} + 9.7\,Na^+ + 10\,H_4SiO_4 \quad (3)$$

Again the compositions of plagioclase and smectite are shown schematically in reaction (3). Reaction (3) serves to illustrate the consumption of Mg and protons, and decreasing K in the fluid phase during the experiment, and the preciptitation of smectite, calcite and silica.

Influence of water/rock ratio upon hydrothermal alteration

The water/rock ratio is an empirical extensive parameter for describing the relative influences of rock and fluid compositions upon the nature of alteration processes during fluid-rock reaction (e.g., Taylor 1979). In hydrothermal experimental studies, the water/rock ratio is usually quantified as the reactant mass of fluid divided by the reactant mass of solid. This definition assumes that the grain-size of starting solids is small enough for all the mass of solids to be available for reaction, which may or may not be true. Not surprisingly, the water/rock ratio has been shown to have a large effect upon the nature of fluid and solid products during hydrothermal reaction (e.g., Seyfried and Bischoff 1977). A water/rock ratio defined by area/volume may be a more meaningful parameter (Lasaga 1984), bearing in mind that silicate dissolution follows zero order kinetics (far from equilibrium), at temperatures up to 200° C, and probably to 700° C (Walther and Wood 1984).

In this study, the water/rock ratio was arbitrarily fixed at an initial value of 10 (by mass) or 3.1×10^{-3} cms (by volume/area), which represents a compromise between a realistic ratio for a low-flow crystalline rock environment and that necessary to permit enough fluid samples to be extracted to monitor reaction progress. The exact volume/area ratios to be encountered in a low temperature ($T < 300°$ C) hydrothermal circulation system in granitic rock is less easy to determine. At one extreme, the volume/area ratio for a zero-flow hydrogeological regime in fractured granite may be considered. Hydraulic testing of the Carnmenellis Granite at a depth of 2 km has suggested an in-situ porosity and permeability of 0.1% and 5 μD. respectively (McCartney, personal communication), which may be interpreted as a fracture spacing of 20 m and a fracture aperture of 5 μm (e.g., Black 1985). A zero-flow groundwater system with such physical characteristics would have a water/rock ratio by volume/area of 5×10^{-18} cm, if the fracture porosity alone is considered. This ratio will increase with increasing flow-rate and with integration through the history of the circulation system, but even so, it is likely that the experimental water/rock ratio used here will theoretically exceed that of a relatively sluggish circulation system. Therefore, it is necessary to consider the influence of this parameter upon potential differences in the alteration observed between the experimental and natural hydrothermal systems.

At low water/rock ratios, the character of hydrothermal alteration products is dominated by the chemical composition of the rock and the prevalent P−T conditions, so that conditions of isochemical metamorphism are approached (Giggenbach 1984). Conversely, hydrothermal alteration at high water/rock ratios leads to the replacement of the rock constituents by chemical components from the fluid and the alteration becomes metasomatic or 'fluid dominated' (Giggenbach 1984). In terms of a comparison between the experimental and natural alteration of the Carnmenellis Granite, then it may be considered that the former should be fluid dominated, whereas the latter should approach isochemical recrystallisation. Since the reactant fluid phase used in the experiments was undersaturated with respect to all starting minerals at the temperatures concerned, and possessed an intrinsically low cation/proton ratio, it may be envisaged that the experiments should show a tendency towards cation leaching of mineral phases, encouraging the growth of kaolinite and calcite ('hydrogen metasomatism' of Giggenbach 1984). Mg metasomatism at all temperatures and Ca metasomatism at 250° C would also be encouraged due to the excess of these elements in the starting fluid as compared with the chemical compositions of the fluids at steady-state, so that the net result of these metasomatic processes would be to produce clay minerals, chlorite and calcite. The presence of smectite clays and calcite in the experimental run products is partial confirmation of these hypotheses although the presence of wairakite at 250° C and laumontite at 150° C (inferred) is a reflection of the alkaline (pH 7–8.5) conditions of the alteration during the experiments due to the rapid titration of fluid acidity through plagioclase dissolution. On the other hand, the alteration of the system at a low water/rock ratio should closely resemble the most thermodynamically stable mineral assemblage for a 'granitic' bulk rock composition at the P−T conditions of alteration. For temperatures less than 250° C, this assemblage may consist of albite, microcline, quartz, muscovite, biotite and laumontite (Giggenbach 1984). Apart from the absence of anorthite (as a component of plagioclase), the hypothetical alteration assemblage for a low water/rock ratio alteration should be broadly similar to the modal mineralogy of the Carnmenellis Granite. In order to compare the theoretical and actual mineral assemblages resulting from water-rock interaction in the Carnmenellis Granite, and also to examine the effect of water/rock ratio upon alteration, a number of vein fillings taken from drillcore from boreholes at the HDR Project Site were investigated (see below).

Comparison with the natural system

Mineralogical examination of the Carnmenellis Granite reveals a continual, episodic history of fluid-rock reaction as indicated by high temperature syn-emplacement features, through to low temperature filling of fractures with clays, zeolites and calcite. A detailed description of the effects of water-rock reaction upon the mineralogy of the Carnmenellis Granite, both in the central and northern zones of the intrusion, is currently in preparation (Bromley et al. in preparation), but a brief summary of the salient features of mineral-fluid reaction in the granite is relevant here.

Figure 11 typifies the features observed from a survey of approximately twenty fine (1–2 mm wide) sealed veins from the Rosemanowes drillcore. Initial, high temperature mineral-fluid reaction is revealed by syntaxial replacement of biotite by muscovite and the sub-solidus growth of tourmaline and potassium feldspar. Synchronous with these features were the alteration of biotite to chlorite and the clouding of feldspars. Further cooling of the granite was accompanied by brittle fracturing and the development of euhedral quartz and optically clear potassium feldspar overgrowths on grains exposed on fracture surfaces. These fractures remained hydraulically active as suggested by the growth of botryoidal masses of high-Fe, then low-Fe smectite-chlorite aggregates, together with a laumontite-calcite assemblage. Kaolinite was not observed or detected in any of the fractures examined. The alteration minerals resulting from the later stages of water-rock reactions observed in the fine vein-fillings bear a close resemblance to the product mineral phases from the hydrothermal experiments and may thus have resulted from water-rock reaction at similar P−T conditions and water/rock ratio. However, it is highly unlikely

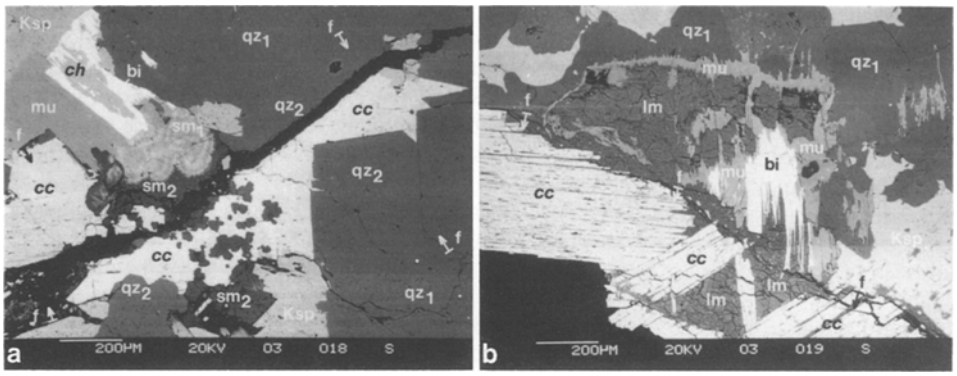

Fig. 11a–b. SEM photomicrographs (backscattered mode) of mineral phases in vein fillings from drillcore from the Rosemanowes HDR test site. The approximate original fracture boundaries are indicated by '*f*' symbols, with *arrows* pointing towards the vein centre. **a** A vein from 2111 m depth showing syntaxial replacement of biotite (*bi*) by muscovite (*mu*) and subsequent alteration of biotite by chlorite (*ch*), high-Fe mixed layer smectite-chlorite (sm_1), then low-Fe smectite (sm_2). Note the euhedral quartz overgrowth (qz_2) on original quartz grains (qz_1) projecting towards the original fracture voidage. Calcite (*cc*) is the other major vein filling phase, Ksp is potassium feldspar. **b** A vein from 2156 m depth showing syntaxial replacement of biotite by muscovite and subsequent replacement of muscovite by laumontite (*lm*). Calcite (*cc*) is the other major vein filling phase. Other symbols as for **a**

that the minerals found in these sealed veins relate to water-rock reaction associated with the current groundwater circulation system. The saline groundwaters of the northern margin of the Carnmenellis Granite occur in much larger fractures, or 'cross-courses' which may be several metres wide (Edmunds et al. 1984). Minerals associated with these fractures include quartz, kaolinite, smectite and illite (Bromley and Thomas 1986), which indicate water-rock reaction at a higher, rather than lower, fluid/rock ratio than that observed or inferred for the autoclave experiments and vein-fillings from the Rosemanowes drillcore.

Although there are many similarities between the chemical compositions of the fluids from the autoclave tests and the Rosemanowes circulation system (Savage et al. 1986), a comparison of the composition of the fluids from the artificial systems with the groundwaters of the Carnmenellis Granite is less rewarding for at least two reasons. Firstly, despite the theoretical considerations discussed above, the mineralogy of the cross courses indicates a much greater water/rock ratio for the groundwater-granite system than that observed in the two artificial systems. Secondly, the groundwater chemistry reflects a summation of all the chemical exchanges identified from the vein fillings in the drillcore from the Rosemanowes test site, as well as probable fluid influx from the surrounding metasedimentary envelope (Bromley and Thomas 1986). A synthesis of the most recent data pertaining to the origin of the saline groundwaters is currently underway (Edmunds et al. in preparation).

Conclusions

The experimental alteration of granite by a dilute meteoric-type fluid under the conditions studied was dominated by the production of mildly alkaline (pH = 7–8.5) fluids of low salinity, together with smectitic clays, calcite and zeolite. Even at the relatively high water/rock ratio employed in the experiments (10:1 by mass), acidity was rapidly titrated, principally by plagioclase feldspar dissolution. The alteration observed in the experiments bears close resemblance to that seen in thin sealed veins at depth in the Carnmenellis Granite, implying similar ambient physical conditions during the later stages of hydrothermal circulation associated with the granite, but is distinct from alteration associated with groundwater bearing cross-courses along the northern margin of the granite. Although kaolinite is generally thought of as the dominant secondary mineral phase replacing plagioclase during low temperature alteration of granitic rocks, this study indicates that kaolinite formation requires a considerably greater water/rock ratio than the considered here, or proton generation by other mechanisms, such as oxidation of sulphide veins in oxygenated shallow circulation systems.

Acknowledgments. The authors would like to thank Dr R.A. McCartney of the Geothermal Energy Project, Camborne School of Mines for fruitful discussions and encouragement throughout the course of this study. Reviews by Drs R.A. Downing, W.M. Edmunds, R.L.F Kay and two anonymous referees improved the manuscript. The authors would also like to thank Ron Collier for editing the manuscript. This research was funded by the UK Department of Energy and the Commission of the European Communities as a component of a broader programme of geochemical studies of granite-water interaction related to Hot Dry Rock geothermal energy development and is published with permission of the Director, British Geological Survey (NERC).

References

Aagaard P, Helgeson HC (1983) Activity/composition relations among silicates and aqueous solutions. II. Chemical and thermodynamic consequences of ideal mixing of atoms on homological sites in montmorillonites, illites and mixed-layer clays. Clays Clay Miner 31:207–217

Batchelor AS (1984) Hot Dry Rock geothermal exploitation in the United Kingdom. Mod Geol 9:1–41

Berner RA, Holdren GR (1979) Mechanism of feldspar weathering. II. Observations of feldspars from soils. Geochim Cosmochim Acta 43:1173–1186

Bischoff JL, Dickson FW (1975) Seawater-basalt interaction at 200° C and 500 bars: implications for origin of sea floor heavy-mineral deposits and regulation of seawater chemistry. Earth Planet Sci Lett 25:385–397

Black JH (1985) The interpretation of slug tests in fissured rocks. Q J Eng Geol 18:161–171

Bourg ACM, Oustriere P, Sureau JF (1985) Experimental investiga-

tion of clogging of fissures and pores in granite. Mineral Mag 49:222–231
Bromley AV, Thomas LJ (1986) A comparitive study of hydrothermal alteration in the Carnmenellis Granite and its metasedimentary envelope. Proc 5th Int Symp Water-Rock Interaction, Iceland, p 83
Chappell BW, White AJR (1974) Two contrasting granite types. Pac Geol 8:173–174
Charles RW (1978) Experimental geothermal loop. I. 295° C study. Los Alamos Sci Lab, Rep LA-7334-M5, p 44
Charles RW, Bayhurst GK (1983) Rock-fluid interactions in a temperature gradient: biotite granodiorite + H_2O. In: Heiken G, Goff F (eds) Geothermal energy from Hot Dry Rock. J Volcanol Geotherm Res 15:137–166
Charoy B (1986) The genesis of the Cornubian batholith (South-West England): the example of the Carnmenellis pluton. J Petrol 27:571–604
Clements RL, Sergeant GA, Webb PJ (1971) The determination of fluorine in rocks and minerals by a pyrohydrolytic method. Analyst 96:51–54
Crossey LJ, Frost BR, Surdam RC (1984) Secondary porosity in laumontite-bearing sandstones. In: McDonald DA, Surdam RC (eds) Clastic diagenesis. Am Assoc Petrol Geol, Tulsa, Oklahoma, USA, pp 225–237
Edmunds WM, Andrews JN, Burgess WG, Kay RLF, Lee DJ (1984) The evolution of saline and thermal groundwaters in the Carnmenellis granite. Mineral Mag 48:407–424
Edmunds WM, Kay RLF, McCartney RA (1985) Origin of saline groundwaters in the Carnmenellis granite (Cornwall, England): natural processes and reaction during Hot Dry Rock reservoir circulation. In: Kitano Y (ed) Water-rock interaction. Chem Geol 49:287–301
Edmunds WM, Kay RLF, Miles DL, Cook JM (1987) The origin of saline groundwaters in the Carnmenellis granite, Cornwall, UK: further evidence from minor and trace elements. In: Fritz P, Frape SK (eds) Saline water and gases in crystalline rocks. Geol Assoc Can Spec Pap 33 (in press)
Fishman MJ, Skougstad MW (1963) Indirect spectrophotometric determination of traces of bromide in water. Anal Chem 35:146–149
Giggenbach WF (1984) Mass transfer in hydrothermal alteration systems – A conceptual approach. Geochim Cosmochim Acta 48:2693–2711
Giggenbach WF (1985) Construction of thermodynamic stability diagrams involving dioctahedral potassium clay minerals. In: Kitano Y (ed) Water-rock interaction. Chem Geol 49:231–242
Helgeson HC (1969) Thermodynamics of hydrothermal systems at elevated temperatures and pressures. Am J Sci 267:729–804
Helgeson HC, Delany JM, Nesbitt HW, Bird DK (1978) Summary and critique of the thermodynamic properties of rock forming minerals. Am J Sci 278:1–229
Holdren GR, Berner RA (1979) Mechanism of feldspar weathering. I. Experimental studies. Geochim Cosmochim Acta 43:1161–1171
Jefferies NL (1984) The radioactive accessory mineral assemblage of the Carnmenellis Granite, Cornwall. Proc Ussher Soc 6:35–41
Lasaga AC (1984) Chemical kinetics of water-rock interactions. J Geophys Res 89:4009–4025
Liou JG (1971) P–T stabilities of laumontite, wairakite, lawsonite and related minerals in the system $CaAl_2Si_2O_8-SiO_2-H_2O$. J Petrol 12:379–411
McCartney RA (1984) Geochemical investigation of two Hot Dry Rock geothermal reservoirs in Cornwall, UK. Unpublished PhD thesis, Camborne School of Mines
Moore DE, Morrow CA, Byerlee JD (1983) Chemical reactions accompanying fluid fluid through granite held in a temperature gradient. Geochim Cosmochim Acta 47:445–454
Moore EL, Ulmer GC, Grandstaff DE (1985) Hydrothermal interaction of Columbia Plateau basalt from the Umtanum flow (Washington, USA) with its coexisting groundwater. In: Kitano Y (ed) Water-rock interaction. Chem Geol 49:53–73
Morrow C, Lockner D, Moore D, Byerlee J (1981) Permeability of granite in a temperature gradient. J Geophys Res 86:3002–3008
Mottl MJ, Holland HD (1978) Chemical exchange during hydrothermal alteration of basalt by seawater. I. Experimental results for major and minor components of seawater. Geochim Cosmochim Acta 42:1103–1115
Sampson B, Fleck A (1984) Measurement of aluminium in dialysis fluid and water by a spectrophotometric procedure. Analyst 109:369–373
Savage D (1986) Granite-water interactions at 100° C, 50 MPa: an experimental study. Chem Geol 54:81–95
Savage D, Cave MR, Milodowski AE (1985) Interaction of meteoric groundwater with Carnmenellis granite at 250° C and 50 MPa: an experimental study. In: High heat production (HHP) granites, hydrothermal circulation and ore genesis. Inst Min Metall, London, pp 315–327
Savage D, Cave MR, Milodowski AE (1986) The origin of saline groundwaters in granitic rocks: evidence from hydrothermal experiments. In: Werme LO (ed) Scientific basis for nuclear waste management, vol 9. Mater Res Soc, pp 121–128
Seyfried WE, Bischoff JL (1977) Hydrothermal transport of heavy metals by seawater: the role of seawater/basalt ratio. Earth Planet Sci Lett 34:71–77
Seyfried WE, Janecky DR (1983) Experimental basalt-solution interaction: implications for the origin of ridge crest hydrothermal fluids. Proc 4th Int Symp Water-rock interaction, Misasa, Japan, pp 433–436
Seyfried WE, Gordon PC, Dickson FW (1979) A new reaction cell for hydrothermal solution equipment. Am Mineral 64:646–649
Stone M (1979) Textures of some Cornish granites. Proc Ussher Soc 4:370–379
Tammemagi HY, Wheildon J (1974) Terrestrial heat flow and heat generation in South-west England. Geophys J R Astron Soc 38:83–94
Tammemagi HY, Wheildon J (1977) Further data on the South-west England heat flow anomaly. Geophys J R Astron Soc 49:531–539
Taylor HP (1979) Oxygen and hydrogen isotope relationships in hydrothermal mineral deposits. In: Barnes HL (ed) Geochemistry of hydrothermal ore deposits. Wiley, New York, pp 236–277
Walther JV, Helgeson HC (1977) Calculation of the thermodynamic properties of aqueous silica and the solubility of quartz and its polymorphs at high pressures and temperatures. Am J Sci 277:1315–1351
Walther JV, Wood BJ (1984) Rate and mechanism in prograde metamorphism. Contrib Mineral Petrol 88:246–259
Watson J, Fowler MB, Plant JA, Simpson PR (1984) Variscan-Caledonian comparisons: late orogenic granites. Proc Ussher Soc 6:2–12
Wilson GC, Long JVP (1983) The distribution of lithium in some Cornish minerals: ion microprobe measurements. Mineral Mag 47:191–199
Wolery TJ (1979) Calculation of chemical equilibrium between aqueous solution and minerals: the EQ3/6 software package. Lawrence Livermore Laboratory, Livermore, California, Rep UCRL-52658, p 41
Zall DM, Fisher D, Garner MQ (1956) Photometric determination of chlorides in water. Anal Chem 28:1665–1668

Received September 3, 1986/Accepted March 3, 1987